Gondwana Research, V. 6, No. 1, pp. 89-105.

ISSN: 1342-937X

GR Gondwana Research

Petrography and Geochemistry of the Carapé Granitic Complex (Southeastern Uruguay)

Leda Sánchez-Bettucci[1], Pedro Oyhantçabal[1], Stella Page[2] and Víctor A. Ramos[2]

[1] *Facultad de Ciencias, Instituto de Geología y Paleontología, Depto. de Geología, Montevideo, Uruguay, E-mail: leda@fcien.edu.uy*

[2] *Facultad de Ciencias Exactas y Naturales, Laboratorio de Tectónica Andina, Universidad de Buenos Aires, Argentina*

(Manuscript received October 22, 2001; accepted September 18, 2002)

Abstract

The southern sector of Uruguay was intruded by numerous granitic plutons during the Brasiliano Cycle. The granites and granodiorites of the Carapé Complex comprise a large part of the Neoproterozoic terrain exposed in southern Uruguay. Typological and age relationships show that the characteristic of the granitic rocks changed during the Brasiliano Cycle. Four groups of granitoids can be distinguished according to their emplacement. The first group corresponds to the Campanero Unit, interpreted as a pre-Brasiliano basement, which includes mainly preorogenic granites. The second group, Pan de Azúcar and related granitoids, includes synorogenic granites and granodiorites. The third granitoid group, Dos Hermanos Granite and related plutons, is classified as late- to postorogenic granites. Finally, the fourth group, consisting of the Águila Granite and related plutons, is represented by alkaline amphibole-biotite granites and are considered as post-collisional alkaline granites, which we assign to an extensional event associated with post-collisional slab-break off marking the end of the late Proterozoic Brasiliano orogenic cycle. Most of the granitic plutons in this area (2,300 km^2) are relatively well exposed and have well-defined intrusive relationships with the metamorphic country-rocks. These granitic rocks are the result of successive magma pulses from similar magma chambers through the late Proterozoic to early Paleozoic times.

Key words: Granitoids, geochemistry, Brasiliano Cycle, Uruguay, petrography

Introduction

The first reference to the granitoids of the Sierra de Carapé area was made by Walther (1927) who described the region as composed of Archean protomylonitic granites and gneisses. Bossi (1983) defined the Carapé Group as a medium- to high-grade metamorphic unit, represented lithologically by mica-schists, amphibolites, marbles and gneisses. This group had its evolution coeval with that of the Lavalleja Group and was considered part of the crystalline basement of the latter (Bossi, 1983). Preciozzi et al. (1985) redefined the Carapé Group as a gneissic-migmatitic complex with granitic intrusions developed between the Lavalleja and Rocha Groups, with ortho- and para-gneisses, amphibolites and migmatites as the main lithotypes.

The Carapé Group as defined by Preciozzi et al. (1985) and Bossi (1983) among others, presents an intricate lithological association comprising medium- to high-grade para-metamorphic rocks (amphibolites and gneisses) and pre- to postorogenic granites. Sánchez-Bettucci (1998) proposed to include the supracrustal metamorphic rocks in the Lavalleja Group and reunited the granitic lithologies into a single unit, the Carapé Complex, based on international stratigraphic criteria (ISG, 1994). On the other hand, due to the great compositional variation and to the scarce geologic, geochronological, and geochemical studies in the area, it is suggested, in this study, to redefine the Carapé Group as the Carapé Granitic Complex. This Complex comprises the syn-, and late- to postorogenic granitoids, emplaced in a pre-Brasiliano Basement (Campanero Unit) composed of preorogenic granites, migmatites and mylonites, and in Brasiliano supracrustals of the Lavalleja Group. In this study we propose that the post-collisional alkaline granites are related to a magmatism that can be linked to the eruptive rocks of the Sierra de Las Animas Complex.

This paper is a preliminary attempt to establish the relationships between the different granitic plutons and granitoid types of southeastern Uruguay, exposed along a belt of about 300 km in a northeast-southwest direction,

and 5 to 40 km in width (Fig. 1). The aim is also to present the regional distribution of different granitoid types related to the main geological structures and to propose a geodynamic evolution for the Brasiliano magmatic belt at these latitudes. In this study, petrographic and geochemical data of 18 granitic plutons are presented. The petrogenesis of these rocks is discussed using all available geochemical data.

Geologic Setting

The Carapé Granitic Complex is exposed between 34°18' and 34°35'S latitude and between 56°09' and 56°23' W longitude in southeastern Uruguay (Fig. 1). It is bounded in the study area by the Lavalleja Group towards the west, and by the Sierra Ballena Shear Zone to the east (Fig. 2).

The Lavalleja Group consists of a late Proterozoic volcano-sedimentary sequence affected by a regional prograde metamorphism developed during the Brasiliano orogeny. Based on petrology, geochemistry and metamorphic grade, a back-arc basin tectonic setting is suggested for the Lavalleja Group (Sánchez-Bettucci et al., 2001).

The Sierra Ballena Shear Zone is a regional NE-trending sinistral strike-slip mega-shear. Fragoso-Cesar et al. (1987) considered it as an intraplate shear zone related to an oblique collision. Fernande et al. (1992) suggested that

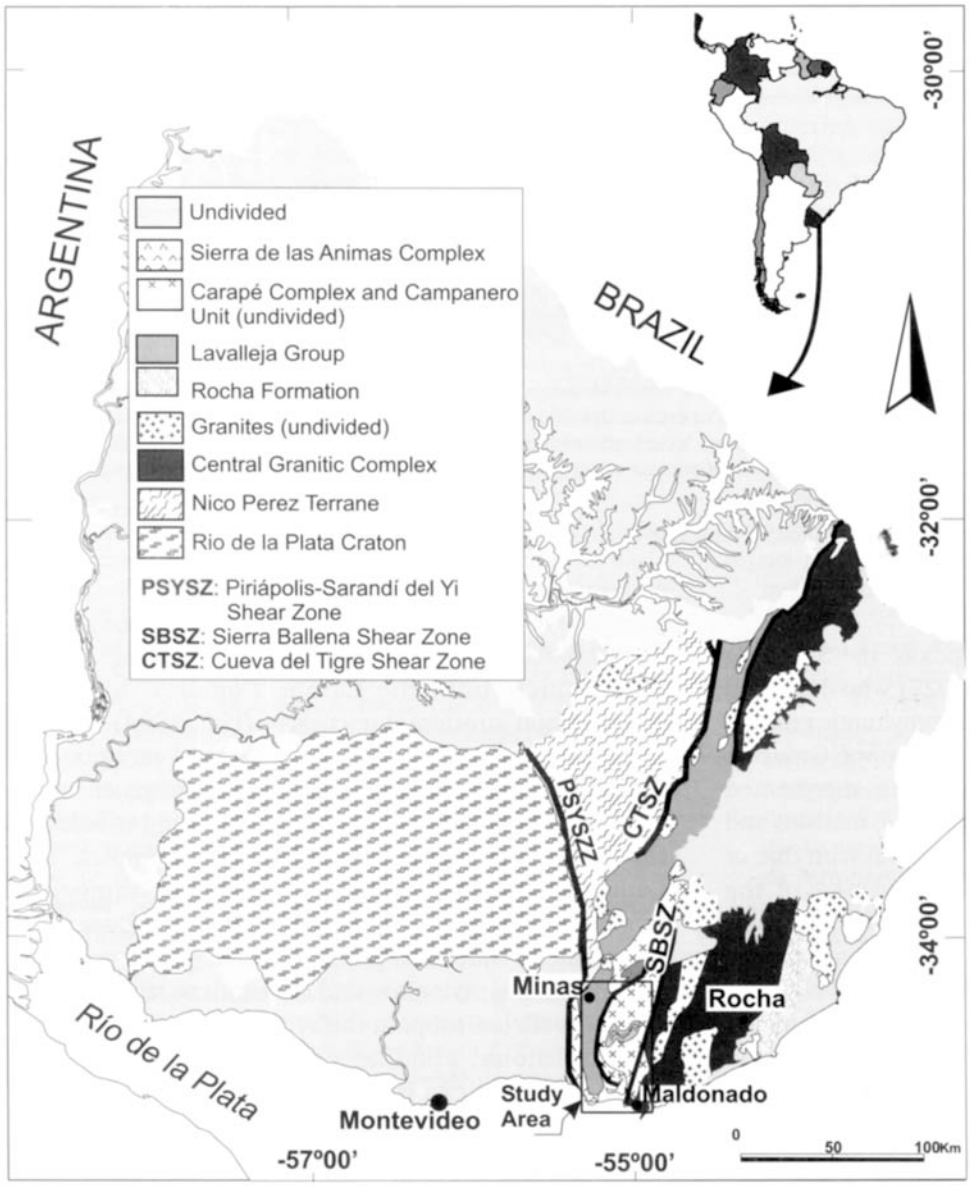

Fig. 1. Location of the study area in a simplified geological map of Uruguay showing the most important Proterozoic units (modified from Sánchez-Bettucci, 1998).

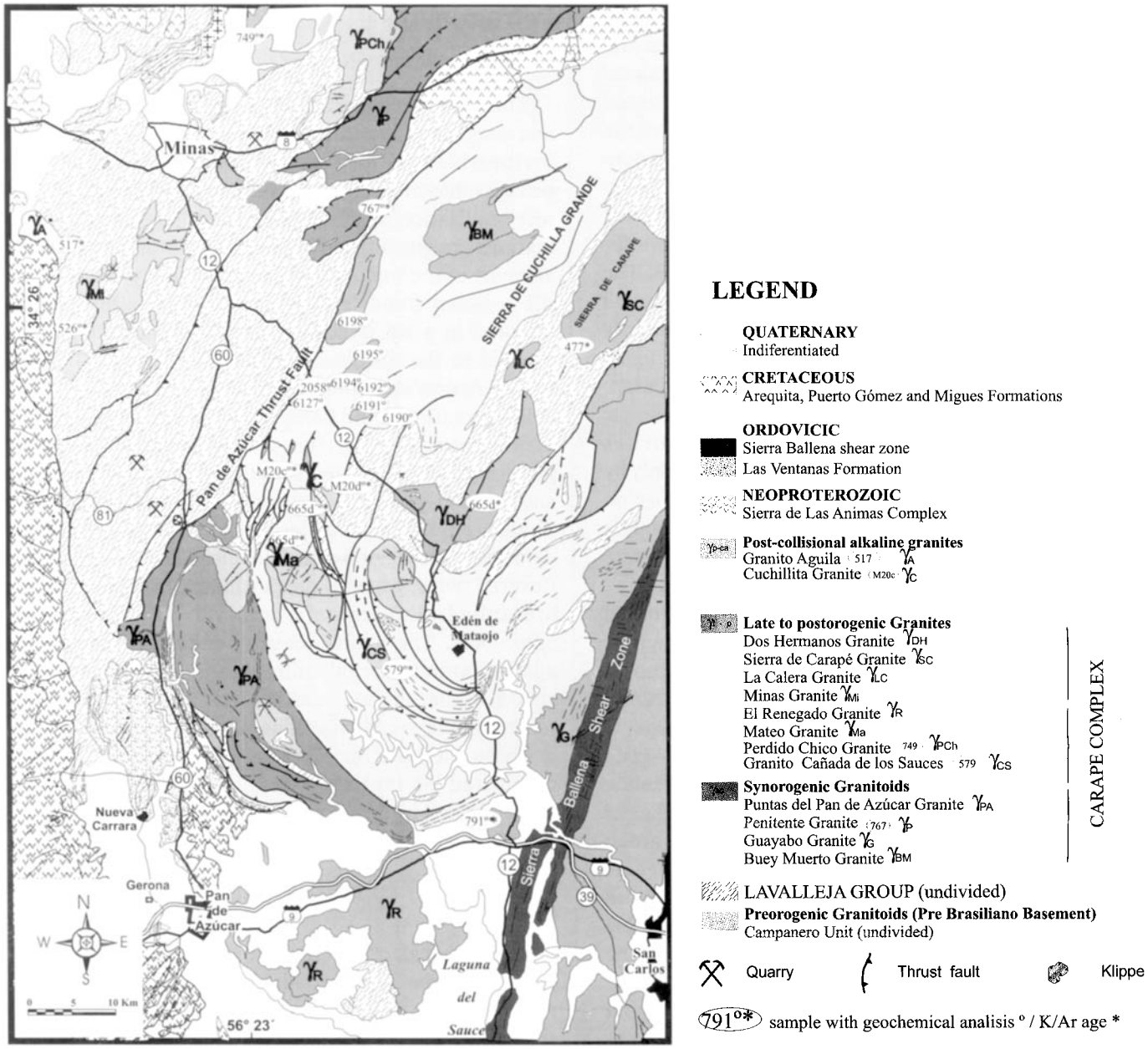

Fig. 2. Geological map of the study area showing the major Neoproterozoic units (simplified from Sánchez-Bettucci, 1998).

this shear zone, known as Dorsal Canguçú in southern Brazil, is the result of late Brasiliano deformation with an important longitudinal transport. Mantovani et al. (1995) pointed out that this unit continues through the Major Gercino Shear Zone. Basei and Teixeira (1987) considered the Major Gercino Shear Zone a crustal discontinuity, and proposed that it represents a suture zone. This shear zone is also characterized by negative gravity anomalies (Mantovani et al., 1995).

The studied plutons are emplaced in low- to medium-grade metamorphosed supracrustals of the Lavalleja Group and in gneisses, protomylonites and mylonites of the Campanero Unit. The plutons have a great variety of exposures, from a few kilometers to 160 km^2. Some of them have oval-shapes, from 0.5 to 1.5 km wide and concordant with the regional foliation, while others are elliptically shaped and discordant with the host-rock. Chilled margins or metamorphic aureoles are not a common feature in the host-rocks. The most frequent colors are light pink to grey and the textures are usually medium-grained and non-porphyric. Textural variations enhanced by deformation are indicated by the local development of mylonitic foliation. Stretching lineations and breccias are frequent structural features due to the

reactivation of the Sierra Ballena Shear Zone. In some cases, the buckling and twinning in plagioclases and biotite sheets, as well as breccia formation and localized foliation development within some plutons can be linked with the activity of this shear zone. The geometry of the original intrusive contacts is obliterated by intense non-coaxial deformation.

The granitoids exposed in the study area can be divided into four main groups based on their field relations, petrography, geochemistry, and structural features. The first group corresponds to the Campanero Unit, interpreted as a pre-Brasiliano basement which includes mainly preorogenic granites characterized by plutons with highly variable composition and little to intense deformation. The second group, Pan de Azúcar and related granitoids, includes synorogenic granites and granodiorites (following Paterson et al., 1989) characterized mainly by their emplacement during the regional deformation period. They exhibit foliation associated with a magmatic flow stage and tectonic foliation related to solid-state deformation as well. The foliation and the stretching lineation, marked by the orientation of biotite and/or amphibole, is normally consistent with that of the host rock. The presence of foliation triple points is a common feature. The third granitoid group, Dos Hermanos Granite and related plutons, is classified as late- to postorogenic granites. Finally, the fourth group, consisting of the Águila Granite and related plutons, is represented by alkaline amphibole-biotite granites, characterized by small plutons discordant with the foliation of the host rock. This group was included in the Carapé Complex as anorogenic granites by Sánchez-Bettucci (1998), but in this work these granites are considered as post-collisional alkaline granites and linked to the genesis of the magma of the Sierra de Las Animas Complex. This Complex, characterized by a bimodal volcanic and subvolcanic suite (Fig. 2), has been assigned to an extensional event associated with post-collisional slab-break off which marks the end of the late Proterozoic Brasiliano orogenic cycle (Oyhantçabal et al., 1993; Sánchez-Bettucci, 1998). It is represented by syenites, granites, trachytes, rhyolites, ignimbrites, basalts and intercalated sediments. Radiometric ages by different methods on different lithologies range from 615 to 500 Ma (Linares and Sánchez-Bettucci, 1997).

The ages of the granitoids can be divided into three groups, the first one includes ages between 540–500 Ma, the second group ranges from 600 to 540 Ma, and the ages of the third group vary between 850 and 750 Ma. The geochronological data from Brazil presented by Soliani (1986), Basei et al. (1997), among others, corroborates these three magmatic stages.

Petrography

Preorogenic granitoids: The Campanero Unit

This unit is represented by a group of heterogeneous and ductile-deformed granitic plutons showing distinct mylonitization and recrystallization. The main petrographic-structural feature is a mylonitic foliation with recrystallization processes (blastesis). The most frequent textures are gneissic, mylonitic, and protomylonitic. The azimuth of the mylonitic foliation is highly variable but the regional trend is 030°. The mylonitic lineation is oriented in a NE trend and subhorizontal plunge sub-parallel to the displacement directions (Fig. 2) of the Pan de Azúcar thrust fault.

The granites of the Campanero Unit are composed of various lithotypes (e.g., fine-grained equigranular biotite granite, medium-grained inequigranular biotite granite, and medium-grained inequigranular biotite leucogranite). These granitoids have undergone grain-scale penetrative deformation. Plagioclase with tabular shape usually shows flexured twins, whereas the perthitic K-feldspars crystals are anhedral. The mafic minerals are biotite and amphibole. The main accessory minerals are sphene, apatite, tourmaline, allanite, garnet (spessartine) and zircon, while sericite, epidote, iron oxides and epidote represent the secondary minerals. Migmatite-like rocks are also included in the Campanero Unit. They are composed of biotite, K-feldspar and quartz, and characterized by distinct segregations of leucocratic and melanocratic domains.

Synorogenic granitoids: Pan de Azúcar and related granitoids

The general characteristic of these synorogenic granites in the area is their emplacement concordant with the regional structures of the host rock (Campanero Unit). The Puntas del Pan de Azúcar Granite and the Penitente Granite are emplaced in tectonic contact with the Lavalleja Group, while the Guayabo Granite is located immediately to the west of the Sierra Ballena Shear Zone. The Buey Muerto Granite (Sánchez-Bettucci, 1998) is located to the southeast of the Penitente Granite (Fig. 2).

The Rb/Sr age of the Penitente Granite is 779±24 Ma (Preciozzi et al., 1993).

They generally present pink to light grey-whitish colors, and vary from fine-grained heterogranular granites with protomylonitic textures to porphyritic leucogranites of shallow emplacements. The accessory minerals are epidote, zircon, and large euhedral garnet crystals (Table 1). The emplacement appears to be closely related to thrusting, resulting in the continuous deformation of

Table 1. Petrographic features of synorogenic granitoids: Pan de Azúcar and related granitoids.

Granites	Puntas del Pan de Azúcar	Penitente	Guayabo	Buey Muerto
Area	160 km²	420 km²	115 km²	80 km²
Color	Pink to gray-pinkish	Pink	Pink	Pink-red
Grain size	Fine to medium	Medium	Medium	Irregular
Texture	Foliated to isotropic	Gneissic (with Qz eyes) to mylonitic (with Qz ribbons)	Mylonitic	Protomylonitic to mylonitic
Mineralogy	Granular Qz in mosaic or ribbons with *undulouse extinction*. Mc up to 4 mm, perthitic intergrowths or partially replaced by Pl, locally myrmekitic textures. Bt, Ms	Qz, Pl , Or, Mc, Bt, KF (mesoperthite, spindle perthite), Sp	KF, Mc, Pl, Qz, Bt, Am	Qz, KF, Pl, Ms, Am Am is progressively replaced by Bt
Accesory minerals	Ep, Zr, Ms, Gt	Om (Mt), Zr, Ep, Gt, Ap	Om, Ap, Ep	Om, Zr, Ep
Secondary minerals	Chloritized Bt, sericitized Pl (Og)	Sericitized Pl	Sericitized Pl, Ep	Sericitized Pl, Ep
Shape of pluton	Irregular	Irregular	Irregular	Irregular
Xenolites, enclaves		Enclaves of medium-grained Bt granite and meter-scale xenoliths of metacalcareous and metapelites partially assimilated, derived from the surrounding basement		

Ab–albite, All–allanite, Am–amphibole, Ad–andesine, Ap–apatite, Arf–arfvedsonite, Au–augite, Aeg–aegirine, Bt–biotite, CPx–clinopyroxene, Cc–calcite, Ep–epidote, F–feldspar, Fa–fayalite, Gt–garnet, Hbl–hornblende, KF–K-feldspar, Li–limolite, Mc–microcline, Mt–magnetite, Ms–muscovite, Og–oligoclase, Om–opaque minerals, Or–orthoclase, Pl–plagioclase, Qz–quartz, Ru–rutile, Se–sericite, Sp–sphene, Tu–tourmaline, Zr–zircon.

Table 2. Petrographic characteristics of late- to postorogenic granitoids: Dos Hermanos and related granites.

Granites	Dos Hermanos	Sierra de Carapé	La Calera	Minas (facies: 1 and 2)	El Renegado (facies: 1, 2 and 3)	Mateo	Cuchillita	Perdido Chico
Area	50 km²	120 km²	120 km²	45 km²	100 km²	50 km²	15 km²	35 km²
Color	Pink	Pink	Pink		Pink, pink-red	Pink	Pink	Pink-gray
Grain size	Fine to medium	Fine to medium	Fine to medium	Fine to porphyritic	1. Border fine-grained 2. Porphyritic, 3. Medium-grained	Fine-grained	Fine-grained	Coarse to medium
Texture	Allotriomorphic inequigranular	Hypidiomorphic inequigranular,	Allotriomorphic inequigranular	1. inequigranular 2. equigranular	Xenomorphic to allotriomorphic equi-inequigranular. Locally granophyric textures	Allotriomorphic inequigranular	Allotriomorphic	Equigranular
Mineralogy	Pl, Qz, Hbl, perthitic F, Bt	Qz, perthitic KF, Mc, Pl, Bt	Qz, perthitic KF, Pl, Bt	1. Bt, 2. Hbl F porphyroclasts, Qz ribbons, Bt Am, Euhedral KF, scarce Og, Qz, Ms, Hbl	1. Qz, perthitic KF, Pl, myrmekite, Bt, Ms. 2. Mc, Qz, Bt, scarce Og, KF phenocrysts up to 3 cm Compositional variations given by presence or not of Am. 3. Pl (An_{26-30}), perthite KF, Qz, Bt, Hbl	KF, Qz, Bt	Qz (triple points, mosaic texture), Ad, red Bt (chloritized), Pl (twinned and flexured), perthitic KF, alk-Am	Qz, Hbl, Pl, KF
Accesory minerals	Om, Zr, Ap	Om	Om, Ms	Zr, Sp, Om	1. Ap, Tu, Om; 2. Zr, Om, Ep; 3. Zr, Ap, Ru	Zr, Om	Ap, Ep, Zr	Ap, Zr
Secondary minerals	Ep, Se	Argillitized and saussuritized Pl, Ep, Se, Li	Argillitized and saussuritized Pl, Ep, Se	Saussuritized Pl	Argillitized and sericitized Pl	Argillitized and saussuritized Pl Ep	Se, Ms, scarce Cc	saussuritized Pl
Shape of pluton	Irregular	Oval	Rectangular *subrounded borders*	Irregular	Irregular	Oval	Oval	Irregular
Xenolites, enclaves				Xenoliths of the Lavelleja Group				Xenoliths of the Lavalleja Group

Abbreviations see table 1.

the granites since the magmatic stage and down into subsolidus conditions. Two small klippes of the Puntas del Pan de Azúcar Granite with an area of 10 km² (Fig. 2) were also recognized. Shear-sense indicators include the following: S-C fabrics, asymmetrical extensional shear bands, rotated porphyroclasts and strain-insensitive foliations. These shear-sense indicators consistently record a sinistral NE-trending sense of shear. Transitions into syn-deformational migmatites are locally observed.

Late to postorogenic granites: Dos Hermanos Granite and related plutons

These granites are epizonal plutons that show discordant contacts with a thermally perturbed host-rock. Two distinct groups of granites have been recognized according to their field characteristics and petrographic and geochemical data: late- and postorogenic granites. The Dos Hermanos, La Calera, and Sierra de Carapé are lateorogenic granites, whereas the Minas, Mateo, El Renegado, Perdido Chico, Cerros Mozos, Piedra del Sombrero and Bombero are classified as postorogenic granites. The general features of these plutons are given in table 2.

The most important feature of the postorogenic granites is that they crosscut all previous structures.

Post-collisional alkaline granites: Aguila Granite and related plutons

Post-collisional alkaline granites are usually related to extension and/or shearing following collision (Sylvester, 1989). It is widely recognized that extension plays an important role in the late stages of orogen evolution, especially during the extensional collapse of orogens (Dewey, 1988). In the study area, these type of plutons are represented by equant-rounded geometries, showing sharp contacts with the host rocks and lacking any deformation. Petrographically, they are characterized by hypidiomorphic textures constituted by coarse-grained K-feldspars (perthitic orthoclase), anhedral quartz occupying interstitial positions, scarce plagioclase, alkaline amphiboles and biotite. The most common accessory minerals are opaques (pyrite), zircon, apatite and sphene. In some samples, myrmekitic intergrowths are observed. The alteration minerals are sericite, calcite, chlorite and epidote.

These plutons were included in the Carapé Complex as anorogenic granites by Sánchez-Bettucci (1998), but are considered in this work as part of Sierra de Las Animas Complex. Small intrusive plutons had been previously recognized and defined as alkaline syenogranites (Oyhantçabal et al., 1993; Sánchez-Bettucci, 1998). The general features of these plutons are given in table 3.

Geochemistry

Analytical techniques

Electron microprobe analysis for major elements and Instrumental Neutron Activation Analyses (INAA) for trace elements were performed at Cornell University. Typical 2σ-precision and 1–5% of accuracy are estimated for major elements (e.g., >1 wt. %) and ~5–10% for minor elements (e.g., <1 wt.%) based on replicate analysis of glass standards. Trace elements analysis by INAA were done on 0.5 g of sample powder packed in ultrapure Suprasil quartz tubing. Ten samples were packed along with three internal standards and irradiated in a TRIGA reactor (Ward Laboratory, Cornell University) at a power level of ~400 kW for 3–4 hours. Samples and standards were counted for 4–10 hours on an Ortec Intrinsic Ge detector; 6 and ~40 days after irradiation. Precision and accuracy (2σ) based on replicate standards analysis is 2–5% for all elements except U, Sr, and Nd which are ~8%. Eight analyses were carried out by Activation Laboratories LTD.,

Table 3. Petrographical features of post-collisional alkaline granitoids: Águila Granite and related plutons.

Granite	Águila	Alkaline syenogranites (undifferentiated)	Cañada de los Sauces
Area	22 km²	5 to 15 km²	8 km²
Color	Red	Gray	Pink
Grain size	Medium- to coarse-grained	Medium to coarse-grained	Medium-grained
Texture	Equigranular	Equigranular	Equigranular
Mineralogy	Qz mosaic textures, Ab with antiperthites, perthitic (vermiform and patches) KF, Bt, Ab, Fa (iddingsite), CPx (Au and Aeg-Au), zoned, scarce alk-Am (Arf)	Perthitic KF, Qz, Ab, Fa (iddingsite), Cpx (subehuedral Au, Aeg-Au), zoned Cpx, Am (Arf)	Ab, KF, euhedral alkaline Am; Qz (<5%)
Accessory minerals	Zr, Ap, All, Ep, Om	Ep, Zr, Om	Sp, Ep
Shape of pluton	Rectangular with subrounded borders	Subrounded	Subrounded

Abbreviations see table 1.

Canada (samples 2058, 6127, 6190, 6191, 6192, 6194, 6195 and 6198). The analytical methods were fusion-ICP for the determination of major elements, and digestion-ICP total and XRF for trace and rare earth elements. Eighteen whole-rock analyses of representative granitoids are given in tables 4a and b.

Results

Major elements: The analyzed samples range from 62.1 to 74.8 wt.% SiO_2.

The data distribution in the $Na_2O + K_2O$ v. SiO_2 (Irvine and Baragar, 1971) diagram shows that 17 samples are subalkaline and only one alkaline (Fig. 3). Further subdivisions were made using the AFM diagram (Fig. 4). The diagram shows a common trend with the granites plotting in the calc-alkaline field.

In the Ab-An-Or diagram (O'Connor, 1965), the samples fall mainly in the granite, granodiorite and trondhjemite fields (Fig. 5). The mobility of certain elements (e.g., Na_2O) and the albitization observed commonly in some samples may explain the shifts towards the trondhjemite field.

On the other hand, the relationships of K_2O v. SiO_2 (Le Maitre, 1989) show a distribution in the medium to high potassium calc-alkaline fields (Fig. 6).

Further attempts to classify the granitoid rocks were made using the diagrams of Maniar and Piccoli (1989). According to this classification (Fig. 7a) the granitoids of the Carapé Complex plot as follows: six samples in the peraluminous field, seven in the metaluminous field, one in the peralkaline (M20c) field and two in the limit metaluminous–peraluminous fields. The peralkaline granite (M20c) is characterized by the presence of olivine (fayalite), pyroxene (aegirine), and alkaline amphibole, while the peraluminous granites are characterized by the presence of garnet, tourmaline, biotite, muscovite, apatite and zircon. Mineralogically, the metaluminous granite contains hornblende, epidote, biotite, and subordinate

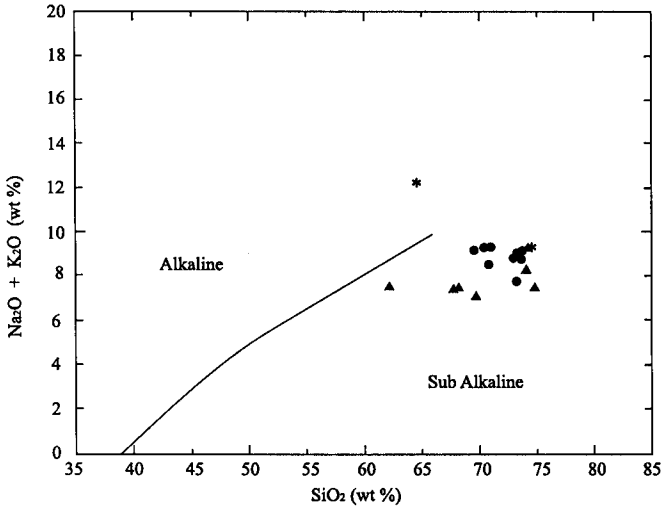

Fig. 3. SiO_2 v. $Na_2O + K_2O$ plot showing the position of the granitoid rocks of the Carapé Complex. Fields after Irvine and Baragar (1971). Symbols: filled circles represent late- to postorogenic granites, triangles represent synorogenic granites, stars represent post-collisional alkaline granites.

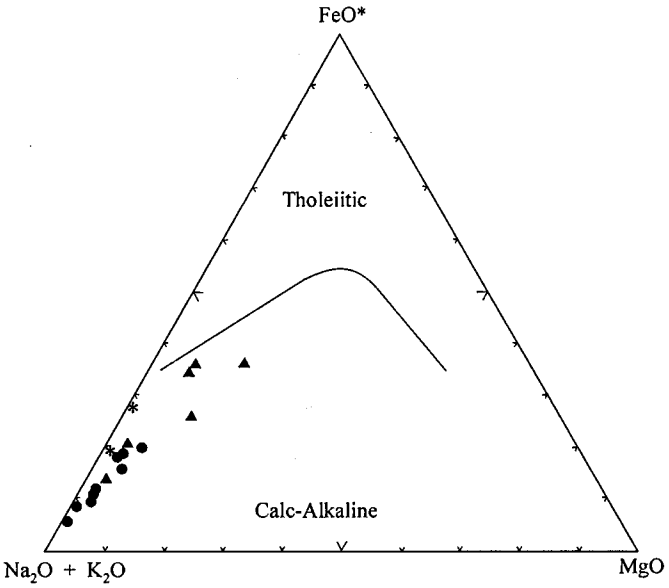

Fig. 4. AFM diagram ($[Na_2O + K_2O]$ - FeO - MgO) for samples of the Carapé Complex. Curved line is the division of Irvine and Baragar (1971) into calc-alkaline (below) and tholeiitic (above) fields. Symbols: filled circles represent late- to postorogenic granites, triangles represent synorogenic granites, stars represent post-collisional alkaline granites.

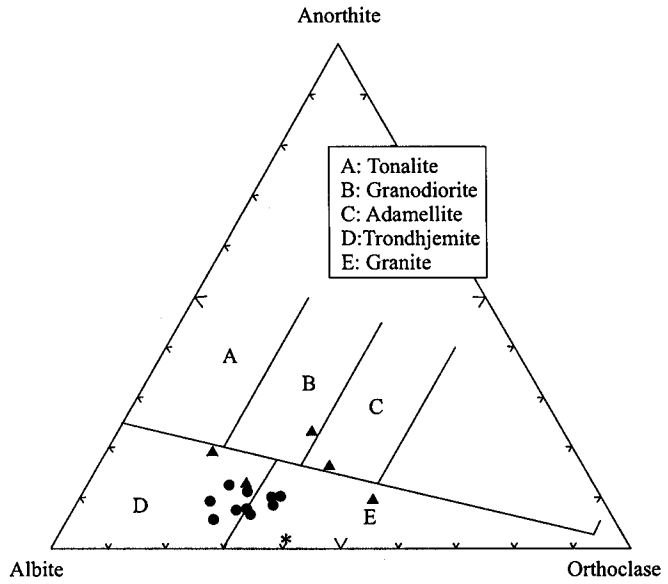

Fig. 5. O'Connor (1965) ternary diagram for the classification of granitic rocks. The granitoids of the Carapé Complex plot in the trondhjemite and granite fields. Symbols: filled circles represent late- to postorogenic granites, triangles represent synorogenic granites, stars represent post-collisional alkaline granites.

Table 4a. Major and trace elements of representative granitoid rocks from the Carapé Complex.

Sample	2058	6127	6190	6191	6192	6194	6195	6198	579	665dï	665d	517	749	791	477	526	M20d	M20c
SiO_2	69.58	72.99	74.24	73.58	73.23	67.72	74.10	68.10	70.91	73.61	73.23	74.63	69.71	70.77	70.37	62.12	74.77	64.58
TiO_2	0.25	0.16	0.06	0.05	0.21	0.90	0.37	0.93	0.18	0.15	0.10	0.16	0.25	0.28	0.33	0.75	0.14	0.34
Al_2O_3	15.50	14.91	15.52	15.31	14.75	13.72	13.21	13.75	16.30	14.68	14.93	13.16	15.48	15.09	15.58	16.31	14.30	16.28
Fe_2O_3	2.33	1.19	0.60	0.91	1.73	4.91	2.55	5.28	1.27	1.00	1.14	2.29	3.00	2.31	2.23	5.78	1.27	4.79
MnO	0.03	0.01	0.00	0.01	0.02	0.09	0.04	0.08	0.01	0.01	0.01	0.01	0.07	0.04	0.08	0.18	0.01	0.19
MgO	0.36	0.26	0.08	0.07	0.49	0.90	0.38	0.96	0.28	0.31	0.32	0.13	1.30	0.71	0.45	2.46	0.29	0.16
CaO	1.60	1.22	0.78	1.10	1.61	2.90	1.25	2.83	1.80	1.06	1.21	0.28	2.98	2.25	1.58	4.56	1.69	1.38
Na_2O	4.69	4.62	5.90	5.06	4.86	3.12	2.81	3.11	6.11	5.20	5.39	4.58	4.90	4.97	4.91	3.48	4.43	6.26
K_2O	4.50	4.20	3.30	3.71	2.92	4.29	5.51	4.36	3.14	3.98	3.66	4.75	2.23	3.55	4.35	4.09	3.09	6.01
P_2O_5	0.14	0.09	0.03	0.02	0.10	0.32	0.09	0.36	0.00	0.00	0.00	0.00	0.07	0.03	0.12	0.27	0.00	0.00
LOI	0.43	0.19	0.24	0.29	0.28	0.40	0.17	0.52	nd	nd	nd	nd	nd	nd	nd	nd	nd	nd
Cr	89	162	134	106	82	130	195	141	10	13	14	14	55	19	5	50	20	3
Ni	63	56	40	36	<15	31	62	67	3	5	2	3	16	5	5	10	2	1
Co	2	3	1	1	3	7	3	5	16	17	26	38	31	12	12	50	37	6
Sc	2	1	<1	2	2	11	4	12	1.70	0.80	0.70	1.70	5.20	3.60	1.40	13.40	1.50	3.80
V	17	14	5	5	21	46	17	54	nd	nd	nd	nd	nd	nd	nd	nd	nd	nd
Cu	<10	<10	<10	<10	<10	<10	<10	18	nd	nd	nd	nd	nd	nd	nd	nd	nd	nd
Pb	47	70	90	40	91	80	57	16	nd	nd	nd	nd	nd	nd	nd	nd	nd	nd
Zn	65	42	<30	<30	59	105	59	61	nd	nd	nd	nd	nd	nd	nd	nd	nd	nd
Bi	0.14	0.16	0.13	0.13	0.22	0.24	0.11	0.13	nd	nd	nd	nd	nd	nd	nd	nd	nd	nd
Sn	3	1	<1	2	1	4	2	3	nd	nd	nd	nd	nd	nd	nd	nd	nd	nd
W	<0.20	<0.2	0.20	0.20	<0.2	0.50	0.30	0.50	nd	nd	nd	nd	nd	nd	nd	nd	nd	nd
Mo	<2	<2	<2	<2	<2	3	3	3	nd	nd	nd	nd	nd	nd	nd	nd	nd	nd
Rb	60	62	42	69	48	103	134	90	nd	nd	nd	nd	nd	nd	nd	nd	nd	nd
Cs	0.3	0.4	0.3	0.8	0.8	0.9	0.5	0.8	0.23	0.65	1.18	8.49	0.98	2.23	0.33	3.85	1.69	0.80
Ba	3100	2470	1920	732	2190	3190	2130	3130	3025	2699	2004	835	985	1022	3623	1235	975	53
Sr	1340	1340	1220	550	2570	695	536	705	1745	1110	1068	260	1118	664	1574	751	424	33
Tl	0.40	0.51	0.44	0.43	0.44	0.79	0.75	0.43	nd	nd	nd	nd	nd	nd	nd	nd	nd	nd
Ga	26.00	22.00	23.00	22.00	19.00	21.00	21.00	20.00	nd	nd	nd	nd	nd	nd	nd	nd	nd	nd
Ta	1.40	0.40	0.40	0.60	0.40	1.90	1.30	1.60	4.30	5.03	4.65	12.91	7.77	3.58	3.70	1.41	10.78	4.84
Nb	18.30	5.60	5.80	5.00	4.70	32.40	22.70	27.00	0.00	0.00	0.00	0.00	0.00	0.00	0.00	0.00	0.00	0.00
Hf	6.20	4.10	2.00	3.40	3.80	15.10	13.90	13.70	4.34	3.56	3.48	14.16	3.77	4.03	7.35	5.63	2.91	14.01
Zr	235	141	51	80	149	655	443	616	nd	nd	nd	nd	nd	nd	nd	nd	nd	nd
Y	15.50	5.90	2.60	4.90	5.90	79.70	33.90	69.50	nd	nd	nd	nd	nd	nd	nd	nd	nd	nd
Th	18.20	9.14	4.63	1.80	9.32	20.50	26.60	19.80	11.00	8.37	6.33	24.98	4.22	4.90	31.94	12.25	2.97	9.99
U	1.42	2.07	1.15	1.53	1.69	2.32	2.08	1.86	2.00	2.57	2.00	4.00	1.10	2.00	4.92	2.56	1.14	2.45
Mg #	23.43	30.20	20.89	13.22	35.94	26.63	22.79	26.47	28.21	35.58	33.34	9.19	43.57	35.39	26.45	43.13	28.92	5.62

Table 4b. Rare earths elements of representative granitoid rocks from the Carapé Complex.

Sample	2058	6127	6190	6191	6192	6194	6195	6198	579	665d'	665d	517	749	791	477	526	M20d	M20c
La	115.0	35.5	4.06	3.80	34.0	241.0	232.0	235.0	12.5	118.0	26.5	74.5	29.7	25.40	94.9	51.4	17.6	129.0
Ce	261.0	62.9	6.6	6.40	56.0	428.0	344.0	391.0	55.2	76.9	49.5	154.8	52.5	49.60	174.0	100.7	35.6	261.9
Pr	22.3	6.7	0.94	0.77	6.41	46.0	30.0	41.7	nd	nd	nd	nd	nd	nd	nd	nd	nd	nd
Nd	82.5	24.8	3.8	2.92	24.0	169.0	91.5	150.0	13.9	72.4	18.6	62.0	23.2	20.50	66.3	35.8	14.1	106.1
Sm	13.1	4.1	1.0	0.69	4.11	25.1	10.7	22.1	3.13	9.75	2.91	11.12	3.76	3.86	10.39	6.82	2.01	14.82
Eu	2.85	1.0	0.28	0.19	1.22	5.52	1.97	4.83	0.91	1.89	0.63	0.97	1.04	0.87	2.11	1.62	0.60	0.65
Gd	7.74	2.79	0.90	0.68	2.89	20.3	8.19	18.2	nd	nd	nd	nd	nd	nd	nd	nd	nd	nd
Tb	0.83	0.29	0.13	0.13	0.30	2.63	1.0	2.31	0.14	0.45	0.09	1.29	0.4	0.35	0.53	0.77	0.14	1.41
Dy	3.34	1.12	0.55	0.74	1.13	13.9	5.48	12.6	nd	nd	nd	nd	nd	nd	nd	nd	nd	nd
Ho	0.49	0.16	0.09	0.16	0.17	2.60	1.05	2.36	nd	nd	nd	nd	nd	nd	nd	nd	nd	nd
Er	1.24	0.40	0.25	0.50	0.49	7.65	3.27	6.98	nd	nd	nd	nd	nd	nd	nd	nd	nd	nd
Tm	0.15	0.05	0.03	0.08	0.05	1.11	0.53	0.99	nd	nd	nd	nd	nd	nd	nd	nd	nd	nd
Yb	0.91	0.32	0.21	0.53	0.39	6.88	3.54	6.26	0.32	0.45	0.11	5.27	1.23	1.02	0.53	2.12	0.31	5.13
Lu	0.14	0.05	0.03	0.08	0.06	1.01	0.62	0.93	0.04	0.04	0.0	0.77	0.19	0.15	0.0	0.31	0.00	0.86
Ce_N/Yb_N	72.9	50.0	8.0	3.1	36.5	15.8	24.7	15.9	43.9	43.5	114.5	7.5	10.9	12.4	83.5	12.1	29.2	13.0
Eu/Eu*	0.80	0.86	0.87	0.82	1.03	0.73	0.62	0.72	nd	nd	nd	nd	nd	nd	nd	nd	nd	nd
La_N/Lu_N	83.4	71.7	14.4	5.1	58.4	24.6	38.6	26.2	33.9	311.8	nd	10.0	16.3	17.8	nd	17.1	nd	15.4
La_N/Yb_N	84.5	74.2	12.9	4.8	58.3	23.4	43.8	25.1	26.1	175.3	161.1	9.5	16.1	16.7	119.7	16.2	38.0	16.8

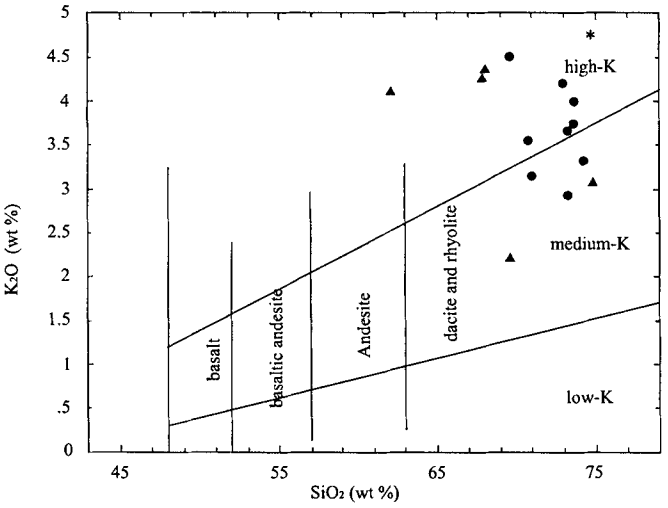

Fig. 6. Diagram of SiO_2 v. K_2O showing the distribution of the high-, medium- and low-K fields (Le Maitre, 1989). The granitoids of the Carapé Complex plot in the medium- and high-K fields. Symbols: filled circles represent late- to postorogenic granites, triangles represent synorogenic granites, stars represent post-collisional alkaline granites.

muscovite, magnetite, apatite and zircon. When the samples are plotted in the Maniar and Piccoli (1989) diagram, they show an erratic distribution (Fig. 7b), although most of them plot in the postorogenic and IAG + CAG + CCG fields.

In the R1/R2 diagram of La Roche et al. (1980) most of the samples plot in the lateorogenic and syn-collisional fields, indicating that their distribution according to different environments (proposed by Batchelor and Bowden, 1985) (Fig. 8), and partially corroborates the petrographic descriptions. The resolution of the diagram in this area is low because it corresponds with a minimum melt composition where all granitoids evolve (Batchelor and Bowden, 1985).

Brown (1982) proposed the arc-maturity using a SiO_2 v. log [CaO/(Na_2O + K_2O)] diagram. The samples of the Carapé Complex plotted in this diagram (Fig. 9) show a relative maturity which corresponds to a normal calc-alkaline magmatism with an extrapolated Peacock's index near 60 wt.% SiO_2.

Minor elements: The concentrations of Sr and Ba show a distribution that could indicate participation of crustal materials (Fig. 10). Bonin (1990) suggested that the relatively high concentrations of Ba and Sr separate the postorogenic from the anorogenic granites, attributing Ba enrichment to the fractionation of alkali feldspar in magmas with low pH_2O. The gradual increase of Ba in relationship to Sr shows that K-feldspar and plagioclase were removed in the differentiation sequence.

Pearce et al. (1984, 1998) proposed that the variation in the content of Ba in within-plate granites is related to

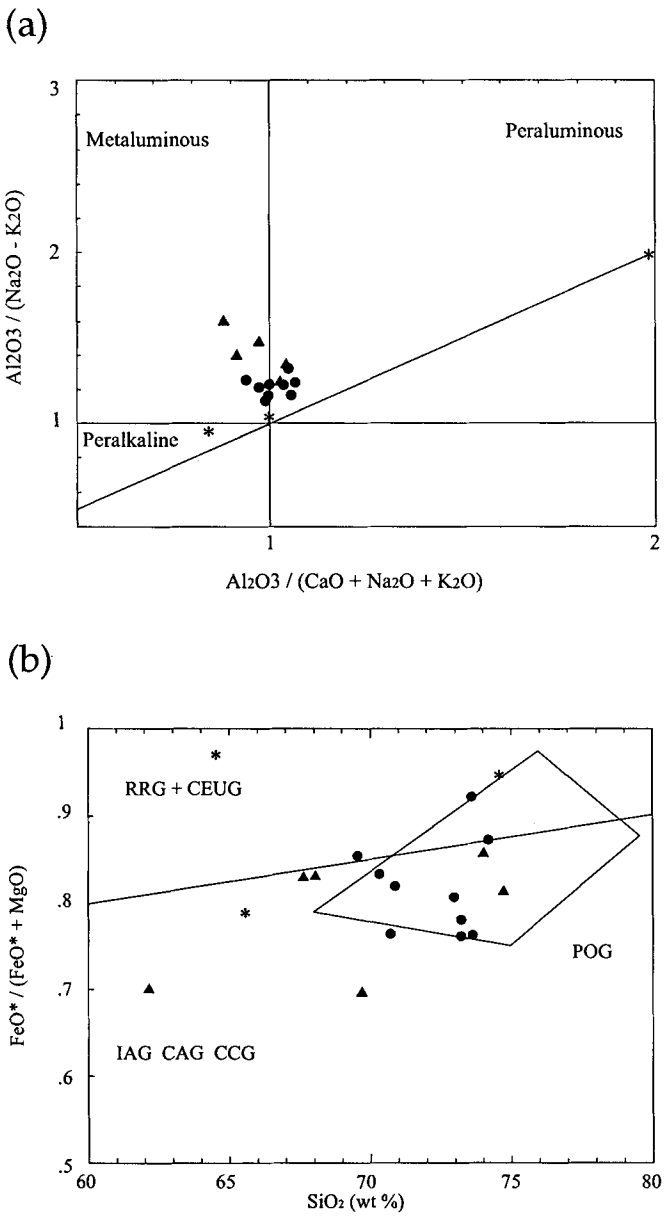

Fig. 7. (a) Shand index for the analyzed samples. (b) Different tectonic settings (Maniar and Piccoli, 1989) based on FeO* /(FeO* + MgO) v. SiO_2 diagram. RRG (rift-related granitoids), CEUG (continental epiorogenic uplift granitoids), IAG (island arc granitoids), CAG (continental arc granitoids), CCG (continental collision granitoids), POG (postorogenic granitoids). Symbols: filled circles represent late- to postorogenic granites, triangle represents synorogenic granites, stars represent post-collisional alkaline granites.

the degree of mantle source enrichment. Figure 10 shows three potential trends; one high in Ba related to Sr, a second trend low in Ba related to Sr and the last one, with low Ba and Sr.

The Nb v. Ba relationship (Fig. 11a) suggests an important crustal influence. Crustal melting under conditions of low pH_2O, related with biotite desequilibrium can generate Ba rich liquids. Ba contents (Fig. 11b) are relatively high

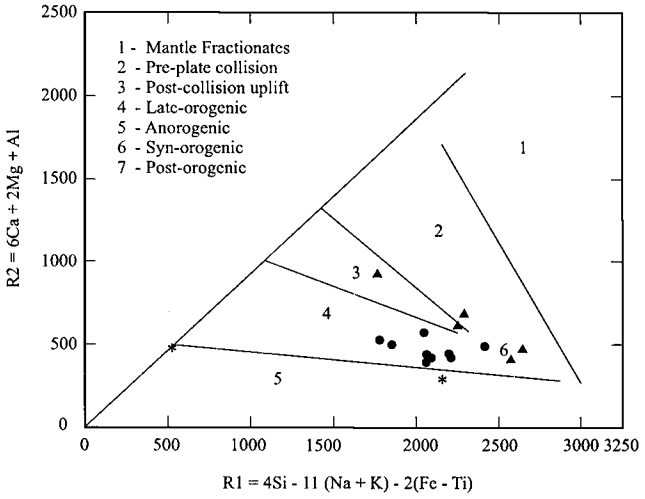

Fig. 8. R1/R2 diagram (La Roche et al., 1980) depicting the different tectonic domains of Batchelor and Bowden (1985) for the granitic rocks of the Carapé Complex. See text for discussion. Symbols: filled circles represent late- to postorogenic granites, triangles represent synorogenic granites, stars represent post-collisional alkaline granites.

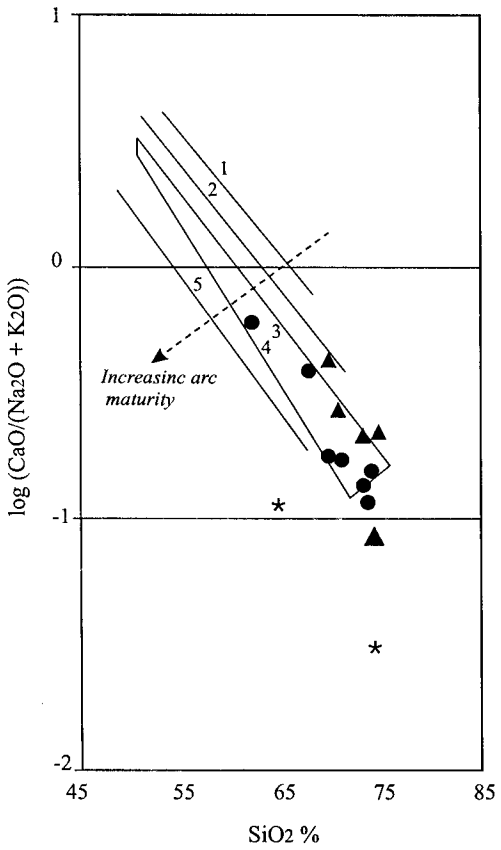

Fig. 9. Plot of the Carapé Complex samples in Brown's (1982) diagram showing relative maturity. Alkali ratio-silica trends for: 1–Tonga S. Sandwich, 2–New Zealand, 3–Field of normal calc-alkaline andesites, 4–Western Americas, Aleutians, Japan, etc., 5–New Guinea. Symbols: filled circles represent late- to postorogenic granites, triangles represent synorogenic granites, stars represent post-collisional alkaline granites.

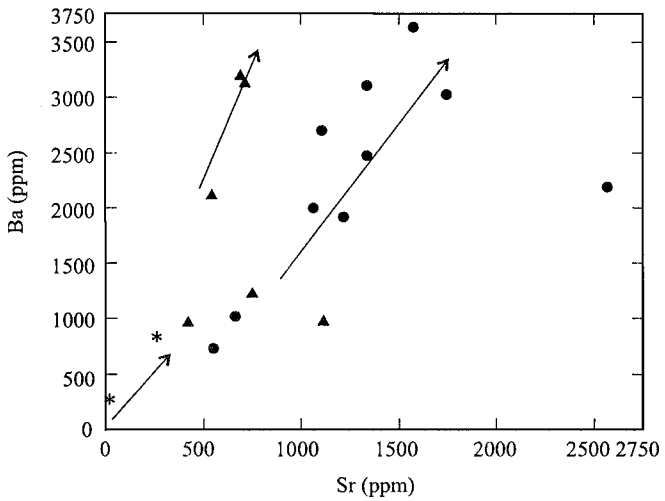

Fig. 10. Sr v. Ba diagram of the Carapé Complex samples showing three different trends. Symbols: filled circles represent late- to postorogenic granites, triangles represent synorogenic granites, stars represent post-collisional alkaline granites.

(>740 ppm except in sample M20c). The Ba behaviour is controlled by several factors, such as the magma alkalinity, source, and the evolutionary history.

Data for Y, Nb, Rb, and Zr are available on eight samples. These samples plotted in the Y + Nb v. Rb diagram (Pearce et al., 1984) show a well-defined cluster in the VAG field and another cluster in the post-COLG field (Fig. 12a). On the other hand, the Y v. Nb diagram (Pearce et al., 1984) illustrates a cluster in the VAG + syn-COLG field and another cluster in the transition between VAG + syn-COLG and anomalous ridge ORG fields (Fig. 12b).

Brown et al. (1984) proposed that the ratios (Ta, Nb)/(K, Rb, La) are not significantly affected by crystal fractionation and can be used to evaluate the arc-maturity. When the granites typified as VAG in figure 12a are plotted in the Rb/Zr v. Y and Rb/Zr v. Nb diagrams (Brown et al., 1984), the samples fall in the intermediate maturity arc region (Fig. 13a and b).

The trivariate plot of Hf-Rb/30-Ta x 3 (Harris et al., 1986) discriminates collisional setting, separated into syn-collisional and late- and post-collisional, within-plate, and volcanic arc. The granites of the Carapé Complex plot in the volcanic arc field (Fig. 14). The post-collisional alkaline granite plot into the within-plate field.

*Rare earth elements:*The chondrite-normalized patterns of REE for the selected rocks of the Carapé Complex are shown in figure 15. The REE patterns suggest a moderate fractionation and in general, they present small negative Eu anomalies except the M20d sample that shows a small Eu positive anomaly. A prominent negative anomaly can be observed in two samples (Fig. 15a).

Three kinds of REE patterns can be recognized. The first type (Fig. 15a) is characterized by REE abundances

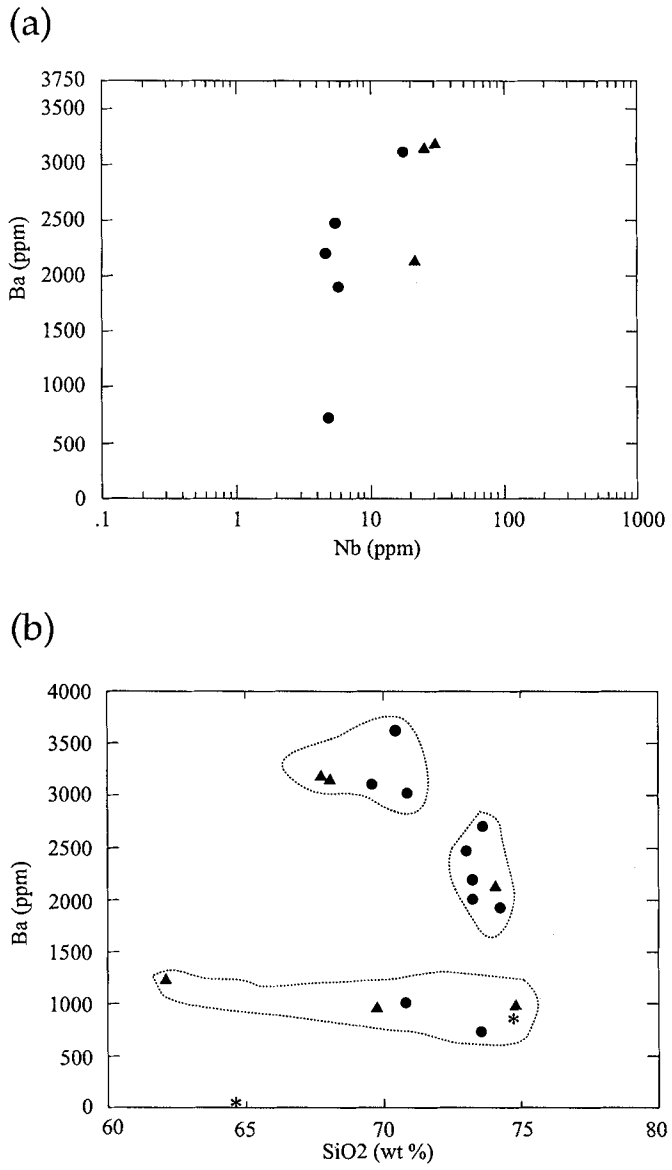

Fig. 11. (a) Nb v. Ba diagram for the analyzed samples. (b) SiO_2 v. Ba diagram. See text for discussion. Symbols: filled circles represent late- to postorogenic granites, triangles represent synorogenic granites stars represent post-collisional alkaline granites.

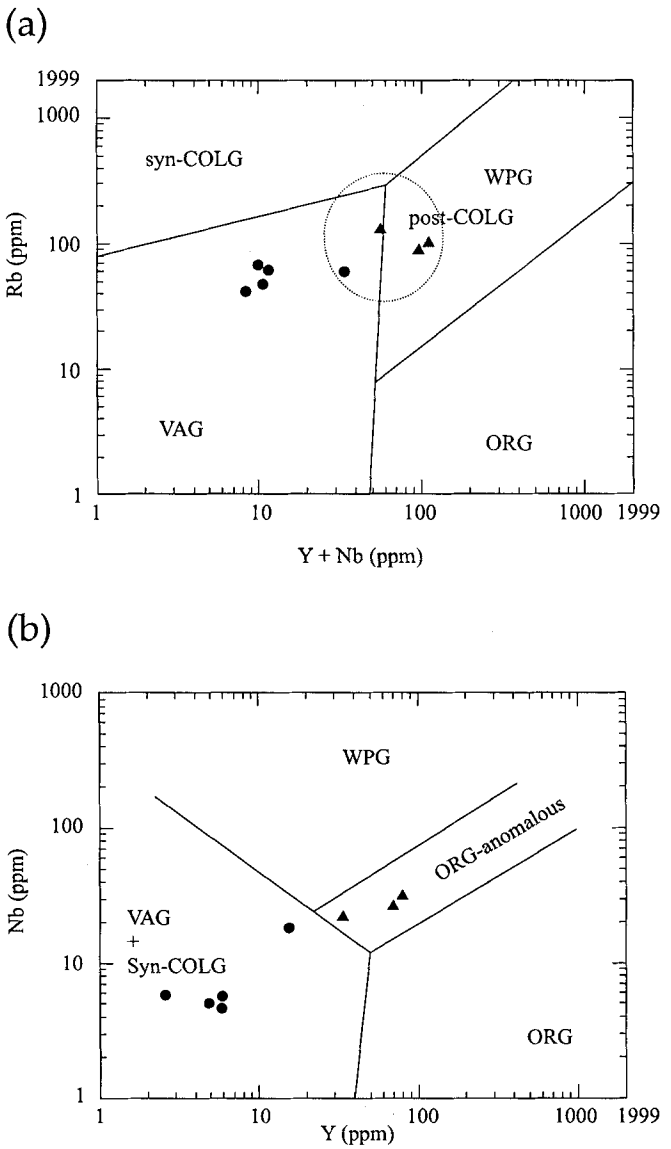

Fig. 12. (a) Analyzed samples in Pearce et al. (1984) diagram, showing a cluster in VAG (Volcanic arc granites) field and another cluster in post-COLG (post-collisional granites). WPG (within - plate granites). (b) Analyzed samples in Pearce et al. (1984) diagram, showing a cluster in VAG + Syn-COLG (Volcanic arc granites + syn-collisional granites) field and another cluster in ORG anom. ridge (Ocean ridge anomalous granites). Symbols: filled circles represent late- to postorogenic granites, triangle represents synorogenic granites.

between 20 and 400 related to chondrite composition (Sun, 1982), low H-REE to L-REE fractionation, and prominent negative Eu anomalies. These samples correspond to the post-collisional alkaline granites (following Sylvester, 1989). The second pattern is characterized by abundances between 1 and 800 related to chondrite composition (Sun, 1982), medium H-REE to L-REE fractionation, and very small or lack of Eu negative anomalies (Fig. 15b), therefore corresponding to post-collisional subalkaline granites. The third pattern, with 0.4 to 110 REE abundances related to chondrite (Sun, 1982), low to medium H-REE to L-REE fractionation, and lack of negative Eu anomalies correspond to volcanic arc granites.

Cullers and Graf (1984) pointed out that positive Eu anomalies could indicate a crustal source with melting of rocks like amphibolites, eclogites or garnet-amphibolites. The crystallization of garnet and amphibole from low differentiated melts can produce positive Eu anomalies and marked fractionation of L-REE relative to H-REE. Lithologies like trondhjemites, tonalities, quartz diorites and granodiorites with negative Eu anomalies commonly present a low absolute content in REE (10.5–144 ppm), and similar L-REE/H-REE ratios (La_N/Lu_N = 5.0–77.5)

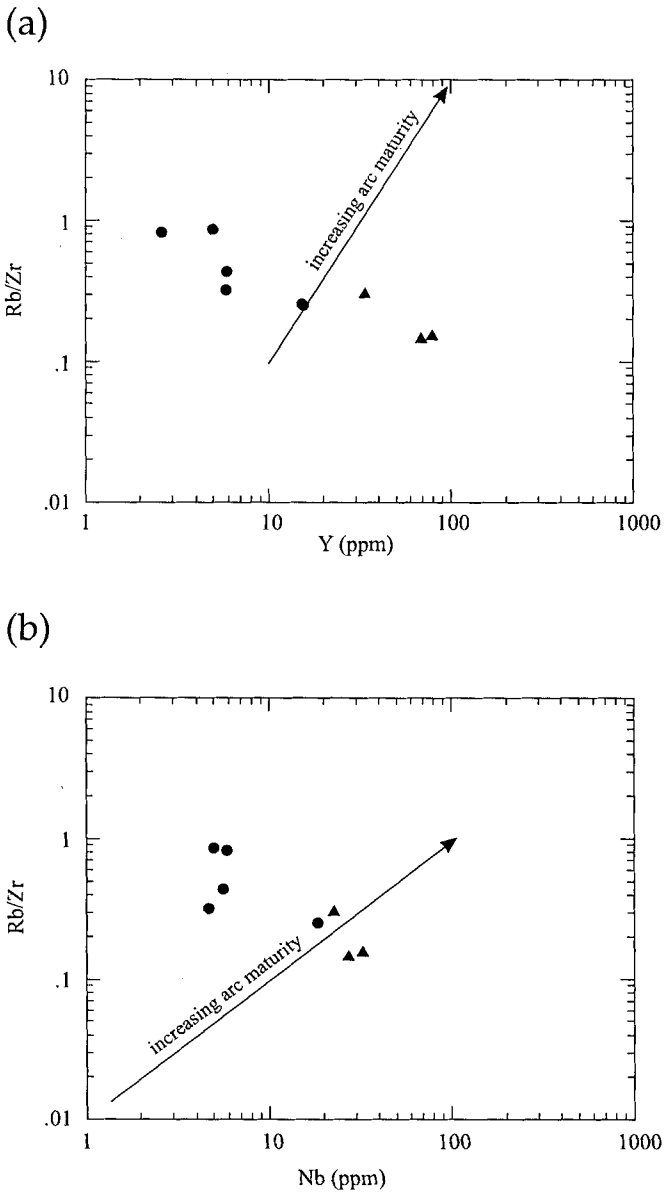

Fig. 13. (a) Rb/Zr v. Y, and (b) Rb/Zr v. Nb diagrams after Brown et al. (1984) showing a normal maturity arc for the Carapé Granitic Complex. In both plots Rb/Zr is higher and Y or Nb lower for late- to postorogenic granites. Symbols: filled circles represent late- to postorogenic granites, triangles represent synorogenic granites, stars represent post-collisional alkaline granites.

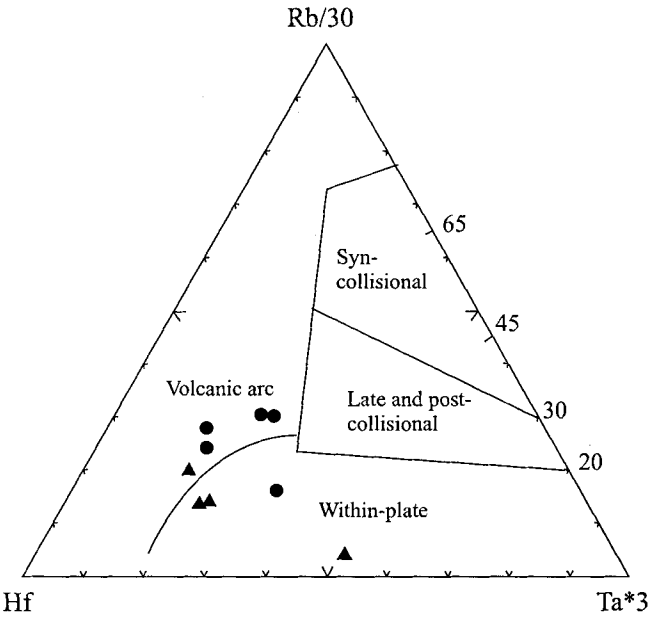

Fig. 14. Triangular Hf-Rb-Ta diagram (Harris et al., 1986) showing the distribution of the Carapé Complex in the Volcanic arc and Within - plate fields. Symbols: filled circles represent late- to postorogenic granites, triangles represent synorogenic granites, stars represent post-collisional alkaline granites.

to that of an island arc (Cullers and Graf, 1984). Rocks with small or without Eu anomaly present moderate to low amounts of REE (between 12 and 273 ppm) and variable L-REE/H-REE ratios. Monzogranites and syenogranites (granites) show REE abundances between 8 and 1997 ppm, while the relationship La_N/Lu_N varies between 0.54 and 137 and Eu_N/Sm_N ratios range from 0.0009 to 1.07 (Cullers and Graf, 1984).

The samples of the Carapé Complex display a La_N/Lu_N ratio between 5.1 and 83.4 except one sample with a value of 311.8, while the Eu_N/Sm_N ratio range from 0.12 to 0.79. The REE abundances range between 0.03 and 428. These features are compatible with monzogranite and syenogranite series.

Age and Correlations

The temporal and geographical distribution of the different types of Brasiliano granitoids provide insights into possible tectono-thermal processes that may have operated in the crust throughout the evolution of the Brasiliano Cycle. In the past, many geologists have speculated that the bulk of the Carapé Granitic Complex could have been related to a magmatic arc, associated with a subduction system and its successive stages (Fragoso-Cesar, 1991; Fernandes et al., 1992). However, new geological and petrologic data have shown that the closure of a back-arc basin is also involved in a more complex history (Sánchez-Bettucci, 1998; Sánchez-Bettucci et al., 2001). The Brasiliano granitic belt in Uruguay has not been studied in detail based on geochemical and geochronological grounds. The geochronological data presented here (Table 5) corresponds to a small portion of the granitoid rocks of the Carapé Complex and only in some cases it is possible to extrapolate. Radiometric ages were determined at the Instituto de Geocronología y Geología Isotópica (INGEIS), using the K/Ar (whole-rock) method. Although the data

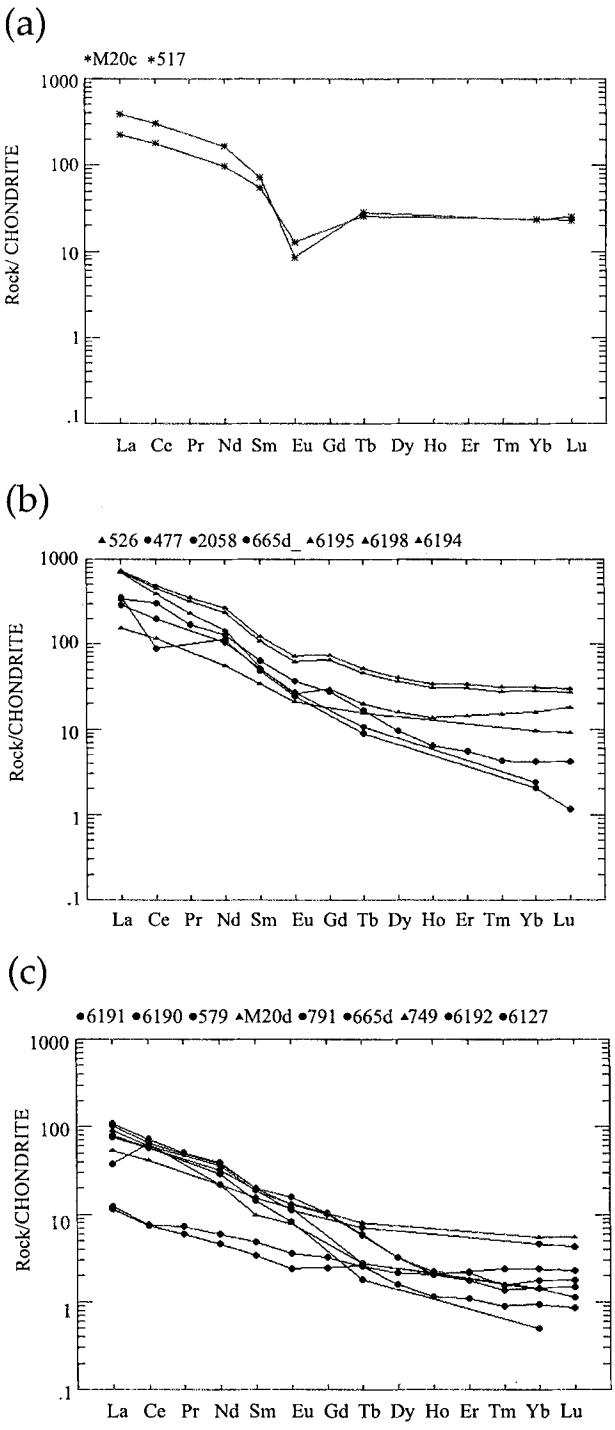

Fig. 15. (a) Chondrite normalized REE variation diagram for the post collisional alkaline granitoids (Sierra de Las Animas Complex) showing very low fractionation and negative Eu anomalies. (b) Chondrite normalized REE variation diagram for the Carapé Granitic Complex, showing medium fractionation and small or absent Eu anomalies. (c) Chondrite normalized REE variation diagram for the Carapé Granitic Complex, showing low fractionation and small or absent Eu anomalies. Sample references are ordered from low to high La content. Normalization constant from Sun (1982). Symbols: filled circles represent late- to postorogenic granites, triangles represent synorogenic granites, stars represent post-collisional alkaline granites.

are limited, they allow distinguishing different magmatic events.

The granitic rocks of the Carapé Complex are correlated with those located in the south of Brazil, which are also part of the Dom Feliciano Belt (following Fragoso-Cesar, 1980). Most of the granitic rocks formed in the Brasiliano Cycle in Brazil are of calc-alkaline affinity with subordinate alkaline occurrences and their compositional evolution can be related to different tectonic episodes associated with the Brasiliano collisional event (Fernandes et al., 1992). The more evolved metaluminous terms were grouped as the Dom Feliciano Granitic Suite (Fragoso-Cesar, 1980). Gastal et al. (1995) suggested that the shoshonitic and alkaline nature is transitional related to postorogenic granites.

The ages of the Carapé Complex granitoids are discriminated into three groups. The first one yields ages from 500 to 540 Ma, while the second gives values of 600–540 Ma. The third group comprises rocks ranging from 750 to 850 Ma. Although the geochronological data are scarce in Uruguay, the granitic rocks in Rio Grande do Sul, southern Brazil, have been extensively dated. The geochronological data from Brazil (Soliani, 1986; Tommasi and Fernandes, 1990; Fernandes et al., 1992; Basei et al., 1997) are consistent with these three groups of ages and, requires the development of significant volumes of granitic magma. Fragoso-Cesar (1991) presented evidences for the existence of Andean-type arc-magmatism in the Pinheiro Machado's calc-alkaline Complex. These calc-alkaline granitic rocks were dated by Rb–Sr method at 770 to 890 Ma (Soliani, 1986; Fragoso-Cesar, 1991). They correlate in Uruguay with the Penitente Granite with a Rb/Sr age of 779±24 Ma, the Aiguá Granite with an age of 582±31 Ma, and the Florencia Granite of 591±95 Ma (Preciozzi et al., 1993).

Preciozzi et al. (1993) outlined the evolution for the Dom Feliciano Belt characterized by four major events. The first one would be represented by low- to high-grade metamorphism of the supracrustal Lavalleja Group responsible for the origin of orthogneisses and migmatites. In this event, the synorogenic granites would have been generated around 880–770 Ma. Shear zones with associated granitoids of ca. 650 Ma represent the second event. The regional framework of the supracrustal rocks was established during this event. The third event is characterized by late-wrenching and postorogenic granitoids with ages varying from 630 to 550 Ma. This event also generated a highly strained zone involving imbricated units. Finally, the fourth event generated late-thrust and post-wrenching granitoids. The existence of a pre-Brasiliano basement is represented by the Campanero Unit, which was recently dated by U/Pb zircon method at

Table 5. K/Ar age of Carapé Granitic Complex.

Sample/Lithology		K %	^{40}K x10^{-8} mol/g	$^{40}Ar_{Rad}$ x10^{-10} mol/g	^{40}Ar-Atm %	Age*** Ma
749:	Perdido Chico Granite*	1.78	5.313	22.367	8.80	609 ± 25
579:	Cda. de los Sauces Granite*	2.42	7.224	24.076	14.20	498 ± 37
517:	Aguila Granite*	3.20	9.552	37.366	9.40	572 ± 12
M20c:	Cuchillita Granite*	3.56	10.627	41.503	18.10	571 ± 10
767:	Campanero Granite*	4.22	12.597	49.278	5.70	572 ± 30
791:	Guayabo Granite**	2.20	6.567	24.334	18.5	546 ± 30

Sánchez-Bettucci and Linares (1999); **this paper; *** Average of two extractions or more appropriate value according to the best isotopic relationships obtained.

around 1.7 Ga (Preciozzi, personal communication, 2002).

The post-collisional alkaline granites may correspond to the same magmatic event as the one that generated the Sierra de Las Animas Complex. This Complex was extruded in late Neoproterozoic to Cambrian times, apparently during a period of about 30–40 Ma, according to available radiometric data (Sánchez-Bettucci, 1998; Preciozzi et al., 1993; Linares and Sánchez-Bettucci, 1997). This data suggests the presence of at least two main phases of magmatism (Sánchez-Bettucci, 1998). One comprises syenites, granites and basalts with an age around 560 Ma and the other includes basaltic flows with a mean age of 547±12 Ma. Therefore, it is interpreted that this phase was erupted approximately between 560 and 540 Ma. Trachytes, rhyolites and dykes represent the younger phase. It is interpreted that this phase of the Sierra de Las Animas magmatism took place at around 520–500 Ma. This long period of magmatism represented by the Sierra de Las Animas Complex is also supported by paleomagnetic results (Sánchez-Bettucci and Rapalini, in press).

Conclusions

The Carapé Complex is an example of felsic magma production through different magma pulses. This Complex has been divided in two groups based on field data such as relationships with the country rock, and petrographic features, as syn- and late- to postorogenic granites. The synorogenic granites display metamorphic penetrative fabrics, whereas the postorogenic and post-collisional alkaline granites crosscut or inherit the structures of the host rock. In most cases, evidence of contact metamorphism was not observed in the host rock, probably because host rock mineralogy was not very sensitive to thermal effects.

The pre-Brasiliano basement (Campanero Unit) is represented by preorogenic granites, migmatites, and mylonites probably of Paleoproterozoic age.

The geochemical characteristics of the different plutons analyzed suggest a transitional setting from volcanic arc to within-plate environments. The granites of the Carapé Complex, characterized geochemically as metaluminous-peraluminous granites with low CaO contents (0.3–4.6 wt.%), high alkalis (7.13–12.27 wt.%) and low to moderate Ba/Sr ratios (0.9–3.2), suggest a calc-alkaline to alkaline tendency with medium- to high-potassium content. The relationships between CaO, Na_2O and K_2O and (Ta, Nb)/(K, Rb, La) show a normal matured arc. The relationship between Nb and Ba suggests a crustal influence probably due to contamination with a pre-Brasiliano basement. Concentratios of Nb, Y, Rb and Zr provide evidence for an evolution from synorogenic through a post-collisional magmatism tectonic setting. The marked depletion in Ba, indicating high K and Sr contents – particularly in one of the samples – is common in arc-related rocks that evolve towards a more alkaline environment in a within-plate continental setting. The chondrite normalized REE diagram shows a moderate fractionation. The negative Eu anomaly is virtually absent in these rocks and the fractionation shown by La_N/Lu_N ratios is moderate to high. The relationship $La_N/Yb_N > 20$ would suggest an emplacement in a thick crust.

Perthitic textures, quartz intergrowths in feldspars, recrystallization of primary phases and neomineralization, present in some of the samples, are interpreted as metamorphic effects during the emplacement and deformation of the plutons.

The post-collisional alkaline granites are related to the magmatism of the Sierra de Las Animas Complex. The REE diagrams of the rocks corresponding to this magmatism show moderate fractionation and a prominent Eu anomaly. This magmatism, characterized as alkaline metaluminous-peralkaline and oversaturated in silica, could have a mantle source, evidenced by the presence of partial melting and crustal assimilation in the evolution of the alkaline basaltic magmas. This process can lead to trachytic liquid and granitic magmas, whereas high Hf contents would also reflect crustal contamination.

Acknowledgments

Research funding by Consejo Sectorial de Investigaciones Científicas (Projects CSIC-078 and CSIC-066), is gratefully acknowledged. We are indebted to S. Kay for the chemical analysis performed at Cornell University. A. Sial, M. Santosh and an anonymous reviewer are acknowledged for substantial suggestions to improve the manuscript.

References

Basei, M.A.S. and Teixeira, W. (1987) Texto explicativo do mapa Geológico do Estado de Santa Catarina 1:500.000, DNPM/CPRM.

Basei, M.A.S., Siga Jr. O., Reis Neto, J.M., Harara, O.M., Passarelli, C.R. and Machiavalli, A. (1997) Geochronological map of the Precambrian terrains of Paraná and Santa Catarina States, southern Brazil: tectonic implications. South-Amer. Symp., São Paulo, Isotope Geol., v. 1, pp. 44-46.

Batchelor, R.A. and Bowden, P. (1985) Petrogenetic interpretation of granitoid rock series using multicationic parameters. Chem. Geol., v. 48, pp. 43-55.

Bonin, B. (1990) From orogenic to anorogenic settings: evolution of granitoid suites after a major orogenesis. J. Geol., v. 25, pp. 261-270.

Bossi, J. (1983) Breve reseña sobre el conocimiento geológico del escudo predevoniano en Uruguay (Sud América). Zeit. Geol. Paläont., v. 1, pp. 417-429.

Brown, G.C. (1982) Calc-alkaline intrusive rocks: their diversity, evolution, and relation to volcanic arcs. In: Thorpe, R.S. (Ed.), Orogenic andesites and related rocks. Wiley, London, pp. 437-461.

Brown, G.C., Thorpe, R.S. and Webb, P.C. (1984) the geochemical characteristics of granitoids in contrasting arcs and comments on magma sources. J. Geol. Soc. London, v. 141, pp. 413-426.

Cullers, R.L. and Graf, J.L. (1984) Rare earth elements in igneous rocks of the continental crust: predominantly basic and ultrabasic rocks. In: Henderson, P. (Ed.), Rare earth element geochemistry, Elsevier, Amsterdam, pp. 237-268.

Dewey, J.F. (1988) Extensional collapse of orogens. Tectonics, v. 7, pp. 1123-1139

Fernandes, L.A.D., Tommasi, A. and Porcher, C.C. (1992) Deformation patterns in the southern Brazilian branch of the Dom Feliciano Belt: a reappraisal. J. South Amer. Earth Sci., v. 5, pp. 77-96.

Fragoso-Cesar, A.R.S. (1980) O Cráton do rio de La Plata e o Cinturão Dom Feliciano no Escudo Uruguaio-Sul-Riograndense. XXXI Cong. Bras. Geol., Camboriú, v. 5, pp. 2879-2892.

Fragoso-Cesar, A.R.S. (1991) Tectônica de Placas no Ciclo Brasiliano: as Orogenias dos Cinturões Dom Feliciano e Ribeira no Rio Grande do Sul. Ph.D. Thesis, Univ. São Paulo, 467p.

Fragoso-Cesar, A.R.S., Machado, R. and Gomez Rifas, C. (1987) Observações sobre o cinturão Dom Feliciano no Escudo Uruguaio e correlações com o escudo do R.G do Sul. III Symp. Sul-Bras. Geol., Curitiba, v. 2, pp. 791-809.

Gastal, M.C.P., Vasquez, M., Gotardo, E., Nardi, L.V.S. and Bitencourt, M.F. (1995) Diversidade composicional entre granitos metaluminosos de afinidade alcalina: exemplos do escudo Sul-Rio-Grandense, R.S. VI Simp. Bras. Geol. e I Encontro de Geol. Cone Sul, Porto Alegre, v. 1, pp. 63-66.

Harris, N.B.W., Pearce, J.A. and Tindle, A.G. (1986) Geochemical characteristics of collision-zone magmatism. In: Coward, M.P. and Riess, A.C. (Eds.), Collision tectonics. Geol. Soc. Spl. Publ., v. 19, pp. 67-81.

International Stratigraphic Guide (ISG) (1994) International Subcomisión on Stratigraphic Classification of IUGS. International Commission on Stratigraphic. Salvador, A. (Ed.), A guide to stratigraphic classification, terminology, and procedure. 214p.

Irvine, T.N. and Baragar, W.R.A. (1971) A Guide to the chemical classification of the common volcanic rocks. Can. J. Earth Sci., v. 8, pp. 523-547.

La Roche, H., Leterrier, J., Grandclaude, P. and Marchal, M. (1980) A classification of volcanic and plutonic rocks using R1-R2 diagram and major element analysis. Its relationships with current nomenclature. Chem. Geol., v. 29, pp. 183-210.

Le Maitre, R.W. (1989) (Ed.), A classification of igneous rocks and glossary of terms. Blackwell, Oxford, 193p.

Linares, E. and Sánchez-Bettucci, L. (1997) Edades Rb/Sr y K/Ar del cerro Pan de Azúcar, Piriápolis, Uruguay. In: South Amer. Symp. Isotope Geol., San Pablo, v. 1, pp. 176-180.

Maniar, P.D. and Piccoli, P.M. (1989) Tectonic discrimination of granitoids. Geol. Soc. Amer. Bull., v. 101, pp. 635-643.

Mantovani, M.S.M., Shukowsky, W. and Hallinan, S.E. (1995) Análise da espessura elástica efetiva no segmento litosférico Rio de La Plata-Dom Feliciano. Anais da Academia Brasileira de Ciencias, v. 67, pp. 199-220.

O'Connor, J.T. (1965) A classification for quartz-rich igneous rock based on feldspar ratios. U.S. Geol. Surv. Prof. Paper, 52SB, pp. 79-84.

Oyhantçabal, P., Derregibus, M.T. and De Souza, S. (1993) Geología do extremo sul da Formaçao Sierra de Animas (Uruguay). In: V Simp. Sul-Bras. Geol., Curitiba, v. I, pp. 4-5.

Paterson, S.T., Tobisch, U.T. and Vernon, R.M. (1989) Criteria for establishing the relative timing of pluton emplacement an regional deformation. Penrose Conference report. Geology, pp. 475-476.

Pearce, J.A., Harris, N.B.W. and Tindle, A.G. (1984) Trace element discrimination diagrams for the tectonic interpretation of granitic rocks. J. Petrol., v. 25, pp. 956 -983.

Pearce, J.A., Keskin, M. and Mitchell, J.G. (1998) Volcano-stratigraphy and geochemistry of collision-related volcanism on the Erzurum-Kars Plateau, northeastern Turkey, J. Volc. Geoth. Res., v. 85, pp. 355-404

Preciozzi, F., Spoturno, J., Heinzen, W. and Rossi, P. (1985) Carta Geológica del Uruguay a escala 1:500.000, Dirección Nacional de Minería y Geología, Montevideo, 92p.

Preciozzi, F., Masquelin, H. and Sánchez-Bettucci, L. (1993) Geología de la Porción sur del Cinturón Cuchilla de Dionisio. In: Field guide, 1 Simp. Int. Neoprot.-Cámbrico Cuenca del Plata. DINAMIGE, Montevideo, pp. 1-39.

Sánchez-Bettucci, L. (1998) Evolución tectónica del Cinturón Dom Feliciano en la región Minas-Piriápolis, Uruguay. Ph.D. Thesis, Universidad de Buenos Aires, 344p.

Sánchez-Bettucci, L. and Linares, E. (1999) New geochronological data of Carapé Complex Granitoids, Uruguay. South Amer. Symp., Córdoba, Argentina. Isotope Geol., v. I, pp. 111-113.

Sánchez-Bettucci, L. and Rapalini, A.E. (in press) Paleomagnetism of The Sierra de Las Animas Complex, Southern Uruguay: its implications in the assembly of western Gondwana. Precamb. Res.

Sánchez-Bettucci, L., Cosarinsky, M. and Ramos, V.A. (2001) Tectonic setting of the late Proterozoic Lavalleja Group (Dom Feliciano Belt) Uruguay. Gondwana Res., v. 4, pp. 395-407.

Solíani Jr., E. (1986) Os dados geocronológicos do Escudo Sul-Rio Grandense e suas implicaçoes de ordem geotectônica. Ph.D. Thesis, Univ. São Paulo, São Paulo, 243p.

Sun, S.S. (1982) Chemical composition and origin of the Earth's primitive mantle. Geochim. Cosmochim. Acta, v. 46, pp. 179-192.

Sylvester (1989) Post-collisional alkaline granites. J. Geol., v. 97, pp. 261-280.

Tommasi, A. and Fernandes, L.A. (1990) O Ciclo brasiliano na porçao sudeste da plataforma sul americana: un novo modelo. Primer Cong. Urug. Geol., v. 1, pp. 107-114.

Walther, K. (1927) Consideraciones sobre los restos de un elemento estructural, aún desconocido del Uruguay y el Brasil más meridional. Bol. 10 Inst. Geol. Perf., 381p.